Biomaterials Science

PAPER

View Article Online
View Journal | View Issue

Cite this: *Biomater. Sci.*, 2020, **8**, 988

Urinary bladder matrix scaffolds improve endometrial regeneration in a rat model of intrauterine adhesions

Honghong Zhang, †[a] Qing Zhang,†[a] Jian Zhang,†[b] Fei Sheng,[a] Shuang Wu,[a] Fu Yang*[c] and Wen Li*[a]

Intrauterine adhesions caused by damage to the basal layer of the endometrium have a serious impact on women's fertility. Currently, there is no effective treatment to promote the regeneration of the endometrium. Urinary bladder matrix (UBM) is a derivative extracellular matrix biomaterial that has a complete basement membrane and provides a basis for the body to achieve complete self-functional repair. In this study, UBM was transplanted into the uterine horns of intrauterine adhesions in Sprague-Dawley rats to test whether UBM could improve endometrial regeneration in rats with intrauterine adhesions. Thicker endometria, increased numbers of glands, fewer fibrotic areas and increased proliferation of cells and blood vessels were found in the UBM group compared to the injury group. Transplantation of UBM reduced the mRNA levels of proinflammatory cytokines (tumor necrosis factor α) and increased those of anti-inflammatory cytokines (basic fibroblast growth factor) compared to the injury group. In the UBM group, the mRNA expression of endometrial receptivity factors (leukemia inhibitory factor and integrin $\alpha V\beta_3$) was higher than that in the injury group, but it was lower than that in the normal group and the sham-operated group. More embryos were seen in the UBM group than in the injury group, although the UBM group had fewer embryos than the normal and sham-operated groups. Therefore, UBM may contribute to endometrial regeneration and may improve endometrial receptivity and fertility.

Received 23rd April 2019,
Accepted 17th September 2019

DOI: 10.1039/c9bm00651f

rsc.li/biomaterials-science

1. Introduction

The endometrium undergoes dynamic, periodic regenerative differentiation during the menstrual cycle, and this regeneration includes the functional layer and the basal layer. A good endometrial environment is important for embryo implantation and normal development and is essential for successful pregnancy.[1] Many conditions, including pregnancy curettage, endometrial polypectomy, submucosal myoma resection, congenital uterine abnormalities, and infections of the reproductive system, can lead to endometrial damage, and severe cases can lead to endometrial hyperplasia, resulting in intrauterine adhesions (IUAs) that affect endometrial receptivity and may lead to recurrent miscarriage and infertility.[2,3] According to the WHO, in the 21st century, infertility will be the disease with the third highest incidence, second only to cancer and cardiovascular diseases, and the current incidence of female infertility in the population is 9% to 18%.[4] According to a report by Evans-Hoeker *et al.*, IUA is a common cause of secondary infertility and accounts for 8% of the cases of infertility.[5] Thus, the effect of IUA on female reproductive function is very significant.

IUA refers to damage of the endometrial basal layer caused by trauma, infection, or other factors. It causes endometrial functional repair disorder leading to endometrial fibrosis.[6] It is also associated with decreased menstrual flow, amenorrhea, recurrent abdominal pain, secondary infertility, recurrent abortion, and placental implantation.[2,7] The main goals of IUA treatment are to reestablish anatomy, treat associated symptoms (including infertility) and prevent the recurrence of adhesions.[8] Currently, the treatment for IUA mainly focuses on hysteroscopic adhesiolysis, prevention of adhesion reformation (by means of an intrauterine device, balloon, hyaluronic acid, or other methods), and improvement of endometrial regeneration by hormone replacement therapy or estrogen administration. However, in severe IUA when the basal layer has been damaged and even when the uterine cavity has been restored

[a]*Reproductive Medicine Center, Second Military Medical University, Changzheng Hospital, 415 Fengyang Road, Shanghai 200003, China. E-mail: liwen@smmu.edu.cn*
[b]*Department of General Surgery, Second Military Medical University, Changzheng Hospital, 415 Fengyang Road, Shanghai 200003, China*
[c]*Department of Medical Genetics, Second Military Medical University, Shanghai 200433, China. E-mail: yangfusq1997@smmu.edu.cn*
†These authors contributed equally to this work.

by surgery, the prognosis remains poor with a recurrence rate of up to 62.5%[2] due to the failure of the functioning endometrial tissue to regenerate. This has been considered as one of the three unresolved clinical problems in regenerative medicine.[9] In addition, the available IUA treatment methods are not perfect; their drawbacks include a long treatment cycle, low pregnancy rates, and high estrogen doses which can increase the risk of breast tumors and endometrial cancer. Therefore, the development of treatment methods that lead to endometrial functional repair is of great significance.

Tissue regeneration is considered to be a promising approach in the treatment of IUA.[10] Biological scaffold materials play a very important role in tissue and organ regeneration, and good clinical results have been achieved using these materials, especially in the areas of severed finger reconstruction, muscle defect repair, wound healing and skin grafting.[11–14] Tissue regeneration provides a new option for the treatment of the endometrium, but it is still in its infancy, and there are only a few reports of its use in this context. The use of an amnion graft is one approach to achieving endometrial regeneration during the treatment of severe IUAs. The amnion graft serves as a biological scaffold and facilitates epithelial cell migration by enhancing basal epithelial cell adhesion and differentiation and preventing apoptosis.[15,16] Lin *et al.* established a rat scarred uterus model in which they transplanted a collagen scaffold to promote the regeneration of the endometrium and muscle, thereby improving pregnancy outcomes.[17–20] Kong *et al.* applied small intestine submucosa (SIS) in a rat IUA model and found that SIS contributed to endometrial regeneration and improved embryo implantation and development.[21] Biomaterials are a new option for endometrial regeneration and repair. However, because many different biomaterials are available, it is essential to identify suitable biomaterials that can be used to improve the treatment efficiency.

Urinary bladder matrix (UBM) is a derivative extracellular matrix (ECM) biomaterial that has a complete basement membrane and can be used to achieve complete self-functional repair.[22] Theoretically, UBM is an ideal material for use in tissue due to its high content of collagens III, IV and VII, elastic fibers, adhesive proteins, and glycoproteins.[23] UBM has been shown to promote regeneration after soft tissue injury through a number of mechanisms. In a clinical study, UBM was shown to promote muscle repair in patients with volumetric muscle loss.[12] UBM has also been applied clinically in cases of chronic non-healing ulcers, resulting in epithelialization of the ulcers with limited scar tissue formation.[13,24] Furthermore, UBM was applied in complicated wounds that were not responsive to conventional therapies, leading to epithelialization and successful skin grafting.[14] UBM was also found to facilitate soft tissue reconstruction in traumatic wounds by establishing a neovascularized soft tissue base.[25] Compared to the amniotic membrane, collagen scaffolds, SIS, and UBM more closely resemble the natural tissue; they exhibit natural resistance to infection, induce tissue regeneration, have ideal mechanical properties and exhibit higher biological activity.[26]

In the present study, we aimed to investigate whether the transplantation of UBM improves endometrial regeneration in rats with IUA.

2. Materials and methods

2.1 Animals

All animal experiments and procedures were approved by the animal experimental ethics committee of the Second Military Medical University, Shanghai, China. Sprague-Dawley (SD) rats weighing 220–250 g were bred in-house in a pathogen-free environment. After allowing the rats to adapt to the environment for one week, vaginal smears were obtained daily between 8:00 and 10:00 AM and were used to evaluate the rats' estrous cycles. Only rats with four consecutive 4–5-day estrus cycles were used in the study. The rats were operated when they were in the diestrus stage.

2.2 Preparation of UBM

UBM derived from porcine urinary bladder was provided by ZhuoRuan Medical Technology Co., Ltd (Suzhou, China). Scanning electron microscopy (SEM) was performed to visualize the surface features of UBM. UBM appears white and consists of soft flakes (Fig. 1A). Under a scanning electron microscope, UBM appears loose and porous, and the three-dimensional structure of its pores is visible (Fig. 1B). Moreover, the material has high porosity and a wide range of pore diameters, features that are conducive to the colonization and proliferation of cells.

2.3 Rat model of IUAs and UMB transplantation

A rat IUA model was established by means of mechanical injury (endometrial curettage using a scalpel blade). Female SD rats were anesthetized with 5% chloral hydrate (6 ml kg^{-1}) by intraperitoneal injection. The uterine horns were exposed through a low abdominal midline incision; the right uterine horn was selected as the experimental side, and the left uterine horn was used as a control. In its upper portion (approximately 0.5 cm from the ovary), the uterus was cut longitudinally with micro-scissors to create an incision approxi-

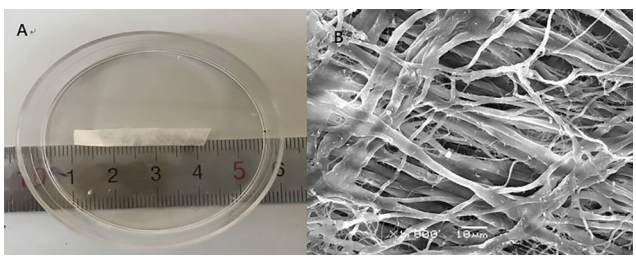

Fig. 1 Appearance and structure of the UBM used in endometrial regeneration. The UBM was very thin; it was 3.0 cm in length, 0.6 cm in width, and 0.1 cm in thickness (A). Scanning electron microscopy showed a scaffold with 1000 μm pore size (B). The scale bar indicates 10 μm.

mately 2.5 cm in length. After the uterine incision, a No. 21 scalpel was used to scrape the endometrium until the uterine wall appeared rough and pale, leaving the mesometrium intact. The uterus was then washed with sterile saline; interrupted sutures were used to suture the uterine incision with 6–0 surgical sutures, and 4–0 surgical sutures were used to suture the abdominal wall muscle and skin tissue. The uteri of the animals were removed two weeks after the operation, and establishment of the intrauterine adhesion model was confirmed by HE staining and Masson staining.

To assess the function of the rat IUA model and the effect of the UBM material on IUAs, 128 uterine horns from 64 rats were randomly divided into four groups. Group A consisted of normal animals that received no treatment (n = 32); Group B was a sham-operated group in which the bilateral uterine horns were exposed through an abdominal incision and incisions and suturing were performed on the uterine horns without scraping the endometrium (n = 32); Group C was a mechanical injury group in which incision, curettage, and suturing were performed on the uterine horns (n = 32); and Group D was the UBM repair group in which surgical scalpel blades were used to scrape the endometrium and the damaged endometrium was then overlaid with a piece of UBM biomaterial (3.0 × 0.6 cm) (n = 32). The other steps used in Group D were the same as those used in Group C. All SD rats were intramuscularly injected with penicillin (80 000 U per 100 mg) daily for 3 days after surgery.

2.4 Histological examination

Sixteen SD rats were sacrificed (8 uterine horns in each group) two, four and eight weeks after surgery, and the uterine horns were removed. Portions of the operative region of the uterine horns were fixed with 4% paraformaldehyde for 48 h and embedded in paraffin. Five-micrometer serial paraffin sections were prepared and stained with hematoxylin and eosin (H&E) and Masson stain. On each H&E section, the thickness of the endometrium was evaluated, and the number of glands was counted in 4 randomly selected fields at 100× magnification. To evaluate endometrial fibrosis, 4 random fields in each Masson-stained section were selected, and the ratio of the endometrial stromal fibrosis area to the total endometrial area was measured using ImagePro Plus software (version 6.0) (Media Cybernetics, USA).

2.5 Immunohistochemistry and immunofluorescence assays

For immunohistochemistry, tissue sections were immunolabeled with antibodies against the von Willebrand factor (vWF, 1 : 10 000, ab6994, Abcam) and Ki67 (1 : 1200, AB9260, Millipore, Billerica, MA, USA). The numbers of capillary vessels and proliferating cells were counted in at least 3 randomly selected fields per section at a magnification of 400×.

2.6 RNA isolation and quantitative real-time polymerase chain reaction

Total mRNA was extracted from uterine tissues using the Trizol method. RNA concentration (OD at 260 nm) and purity ($OD_{260/280}$) were measured using a Nano Drop 2000c spectrophotometer (Thermo Scientific, Bonn, Germany). When the $OD_{260/280}$ ratio of the obtained RNA was 1.8–2.0, the sample was selected for use. One microgram of total RNA from each sample was reverse-transcribed to generate cDNA. First-strand cDNA was generated using the PrimeScript RT reagent kit according to the manufacturer's instructions (Takara Bio, Japan) on an Applied Biosystems Veriti96 system (Applied Biosystems, America). The thermocycler protocols used for reverse transcription were 15 min at 37 °C, 5 s at 85 °C and ∞ at 4 °C.

Subsequently, relative quantitative real-time polymerase chain reactions (qRT-PCR) were performed using 96-well optical plates and analyzed using the Applied Biosystems 7500 Fast Real-Time PCR Detection System (Applied Biosystems). Each gene and sample were assayed in triplicate. In a total volume of 20 μl, each well contained 10 μl of 2 × SYBR® Premix EX Taq™, 1 μl of cDNA, 0.5 μl of forward primer (10 mmol L^{-1}), 0.5 μl of reverse primer (10 mmol L^{-1}) and 8 μl of RNase-free ddH_2O. The primer sequences used for each target gene are shown in Table 1. The cycling parameters for the qRT-PCR were as follows: initial denaturation at 95 °C for 15 min followed by 40 cycles of 15 s at 95 °C, 15 s at 60 °C and 20 s at 72 °C. Analysis of the relative gene expression was performed using the 2-ΔΔCT method. Relative messenger RNA (mRNA) expression is given as fold change relative to untreated controls after normalization to the expression of glyceraldehyde phosphate dehydrogenase, a housekeeping gene.

2.7 Function testing

The function of the regenerative endometrium was assessed by testing whether it was receptive to a fertilized ovum and could support an embryo to the late stage of pregnancy. Eight weeks post-procedure, thirty-two rats were mated. The day of vaginal plug appearance was considered as gestational day 0. Sixteen rats were euthanized at day 5 of gestation, and their uterine horns were used to assess endometrial receptivity. Sixteen rats were euthanized at gestational days 17–19, and their uteri were examined for the presence of embryos.

2.8 Statistical analysis

GraphPad Prism 6.0 software was used to analyze and graph all of the data. Comparisons between the general characteristics and pregnancies in each group were performed using the chi-square test. One-way ANOVA and Student's t-test were performed to compare endometrial thickness, number of glands, fibrotic areas of the uterine horns, and mRNA expression of cytokines. Differences were considered significant at $P < 0.05$.

3. Results

3.1 Postoperative uterine morphology

4 weeks after surgery, the uteri of 16 rats were observed by laparotomy. We found that all of the experimental groups had adhesions to the surrounding tissues in the operative regions

Table 1 Primers of specific genes used in qRT-PCR analyses

Gene	Forward (5′–3′)	Reverse (5′–3′)
VEGF	TACTGCTGTACCTCCACCAT	GGGTACTCCTGGAAGATGTC
B-FGF	GATCCCAAGCGGCTCTACTG	TCGCACACACTCCCTTGATG
TGF-β	GCTGGAGAAGCAGAGTCGTC	CACACCCCACAGAACTTAGC
TNF-α	GTGCCTCAGCCTCTTCTCATT	CATTTGGGAACTTCTCCTCCTT
TIMP	CGCTAGAGCAGATACCACGA	AGCGTCGAATCCTTTGAGCA
PDGRBB	TGACCACTCCATCCGCTCCT	CCAGAATGTGCTCGGGTCAT
COLIA1	CCCTGAAGTCAGCTGCATA	GGCAGAAAGCACAGCACTC
RUNX	TACCCACGGCAAGTTCAACG	CACCAGCATCACCCCATTTG
Integrin $\alpha V\beta_3$	GTGAAGAAACAGAGCGTGTCC	GAGGCAGAGTAGTGGTTGTCG
LIF	GCTGAGGAGTGCTGAAACATC	ATCCCACTGCTGAACTGCTAA
GAPDH	TACCCACGGCAAGTTCAACG	CACCAGCATCACCCCATTTG

except the normal group, and the adhesions in the injury group were more severe. Some uterine horns developed distal hydrometra caused by intratubal obstruction (Fig. 2). The hydrometra rates in the normal group (0%), the sham-operated group (25%), and the UBM group (31.25%) were lower than the hydrometra rate in the injury group (81.25%). In the UBM group (31.25%) and the sham-operated group (25%) the hydrometra rates were similar, but they were higher than that in the normal group (0%) (Table 2).

3.2 Histological examination analysis

By H&E staining (Fig. 3A and B), we observed that two weeks after the surgery, the UBM biomaterial was not completely degraded. We could see a large amount of undegraded UBM material in the uterine cavity as indicated by the arrows in Fig. 3A. Four weeks after the surgery, the UBM biomaterial appeared almost completely degraded. In H&E stained sections, we could hardly see any residual UBM material (Fig. 3B).

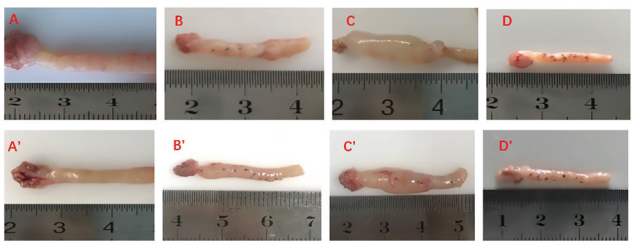

Fig. 2 Gross view of reconstructed uterine horns at 2 weeks (A to D) and 4 weeks (A′ to D′) post-operation in the normal group (A and A′), the sham-operated group (B and B′), the injury group (C and C′) and the UBM group (D and D′). Hydrometra rates of the uterine horns are presented in Table 2.

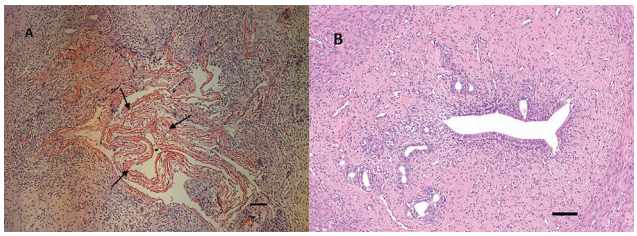

Fig. 3 Histological structure of the uterine horns at 2 weeks (A) and 4 weeks (B) in the UBM group (H&E ×100). Undegraded UBM is marked with arrows in (A) and hardly any residual UBM material can be seen in (B). The scale bar indicates 100 μm.

The epithelium was analyzed by H&E staining (Fig. 4A–D). At 4 weeks after surgery, the uteri of all groups were lined with a simple columnar epithelium that was similar to the epithelial lining of the normal uterus. There was more apparent cellularization in the UBM group than in the injury groups. The thickness of the endometrium in the UBM group (565.2 ± 107.5 mm) was higher than that in the injury group (231.1 ± 136.2 mm) and similar to that in the normal (705.2 ± 77.4 mm) and sham-operated (697.4 ± 159.4 mm) groups (Fig. 4E). The number of glands in the endometrium in the UBM group (12.7 ± 1.9) was higher than that in the injury group (4.7 ± 1.6) and similar to that in the normal (15.3 ± 2.8) and sham-operated (13.13 ± 2.64) groups (Fig. 4F).

We also assessed fibrosis after different treatments (Fig. 5A–D) by Masson staining. We found that at 4 weeks after surgery the percentage of the fibrotic area in the UBM group (40.0 ± 14.4%) was lower than that in the injury group (82.5 ± 14.7%) and similar to that in the normal (32.8 ± 9.1%) and sham-operated (36.1 ± 9.5%) groups (Fig. 5E).

Table 2 Hydrometra rates of uterine horns[a]

	Normal group (n = 16)	Sham-operated group (n = 16)	Injury group (n = 16)	UBM group (n = 16)	P value
Hydrometra (%)	0 (0)[b]	4 (25)[c]	13 (81.25)	5 (31.25)[d]	$P < 0.01$
No hydrometra (%)	16 (100)	12 (75)	3 (18.75)	11 (68.75)	
Total	16 (100)	16 (100)	16 (100)	16 (100)	

[a] n indicates the number of uterine horns. Bonferroni correction: critical level of significance, $p < 0.01$. [b] $p < 0.01$, normal group *versus* injury group. [c] $p < 0.01$, sham operated group *versus* injury group. [d] $p < 0.01$, UBM group *versus* injury group.

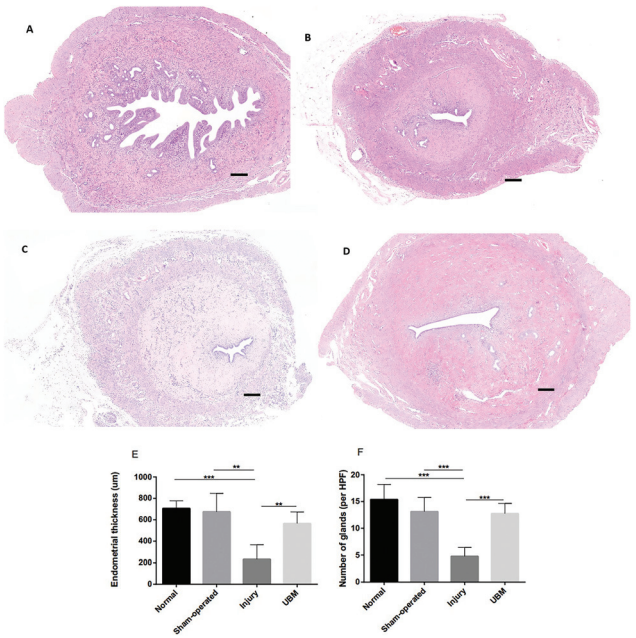

Fig. 4 Histological structure of the uterine horns at 4 weeks (A to D) in the normal group (A), the sham-operated group (B), the injury group (C) and the UBM group (D) (H&E ×50). The scale bar indicates 200 μm. Statistical analyses of the thickness of the endometrium (E) and the number of glands (F) show that the thickness of the endometrium in the UBM group was higher than that in the injury group and similar to that in the normal and sham-operated groups and that the number of glands in the UBM group was greater than that in the injury group and similar to those in the normal and sham-operated groups. The data are presented as the mean ± SD; $^{**}p < 0.01$ and $^{***}p < 0.001$.

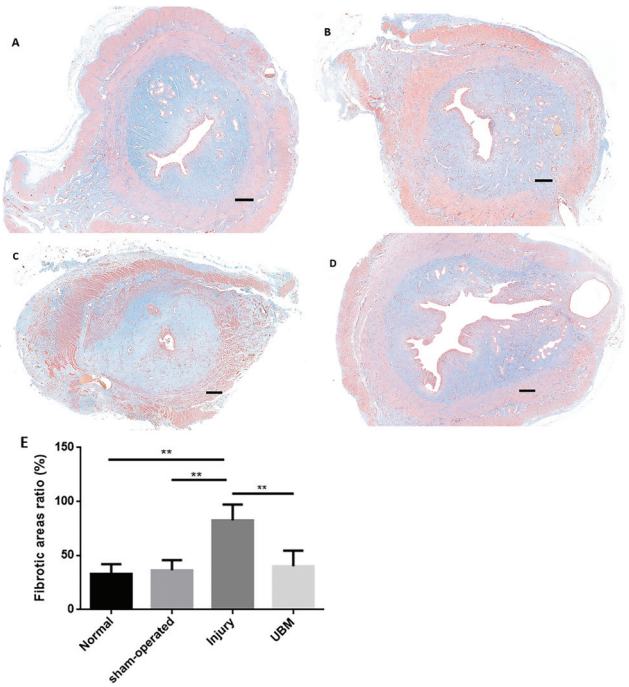

Fig. 5 UBM transplantation reduces injury-induced fibrosis. Masson's trichrome staining of the collagen at 4 weeks (A to D) in the normal group (A), the sham-operated group (B), the injury group (C) and the UBM group (D) (Masson's trichrome staining ×50; the scale bar indicates 200 μm). (E) Statistical analysis of the fibrotic areas indicated that the fibrotic area in the UBM group was smaller than that in the injury group and similar to the fibrotic area in the normal and sham-operated groups. The data are presented as the mean ± SD; $^{**}p < 0.01$.

3.3 Immunohistochemical staining of the uterine horns

3.3.1 Cell proliferation of the endometrium. Ki67 is a nuclear antigen that is used to detect cell proliferation at all stages. During wound repair, normal cells migrate to the damaged area, proliferate, and contribute to the wound repair. Here, we perform immunohistochemical staining of Ki67 to determine whether UBM promotes endometrial cell proliferation (Fig. 6A–D). At 4 weeks after surgery, the number of proliferating cells found in at least 3 randomly selected fields at a magnification of ×400 was calculated. Only a small number of proliferating cells (25.5 ± 7.4) were found in the endometrium of the injury group, while the number of proliferating cells in the UBM group (46.4 ± 6.9) was significantly higher and was similar to the number of proliferating cells in the normal group (42.9 ± 10.2) and the sham-operated group (36.8 ± 4.3) (Fig. 6E).

3.3.2 Blood vessels of the endometrium. We performed immunohistochemical staining to assess the distribution of blood vessels in the endometrium after UBM transplantation (Fig. 7A–D). At 4 weeks after surgery, the number of blood vessels found in 3 randomly selected fields at a magnification of ×400 was calculated. We found that the number of blood vessels in the UBM group (13.4 ± 3.8) was significantly higher than that in the injury group (7.4 ± 1.3) and similar to that in the normal group (14.7 ± 1.4) and the sham-operated group (13.2 ± 2.5) (Fig. 7E).

3.4 Effects of UBM transplantation on cytokine gene expression

At 2 weeks after surgery, the mRNA levels of the anti-inflammatory cytokine basic fibroblast growth factor (b-FGF) were significantly upregulated in the uterine tissue in the UBM group compared to the injury group, the normal group and the sham-operated group, whereas the expression of the proinflammatory cytokine tumor necrosis factor α (TNF-α) was significantly decreased in the uterine tissue in the UBM group compared to the injury group (Fig. 8A).

Consistently, at 4 weeks after surgery, bFGF expression increased and TNF-α expression decreased in the uterine tissue in the UBM group compared to the normal group, the sham-operated group and the injury group. At 4 weeks after surgery, the bFGF level was also increased in the uterine tissue in the injury group compared to that in the normal group (Fig. 8A).

At 2 weeks after surgery, the mRNA levels of the profibrotic cytokines transforming growth factor-β (TGF-β), tissue inhibitor of metalloproteinase (TIMP), platelet-derived growth factor (PDGF)-BB and collagen type I alpha 1 (COL1A1) were significantly increased in the injury group compared to the normal and sham-operated groups. Furthermore, the expression of these cytokines was significantly downregulated in the UBM group compared to the injury group ($P < 0.01$, $P < 0.01$, $P < 0.0$, and $P < 0.05$, respectively; Fig. 8B). These cytokines showed a similar expression trend 4 weeks after surgery.

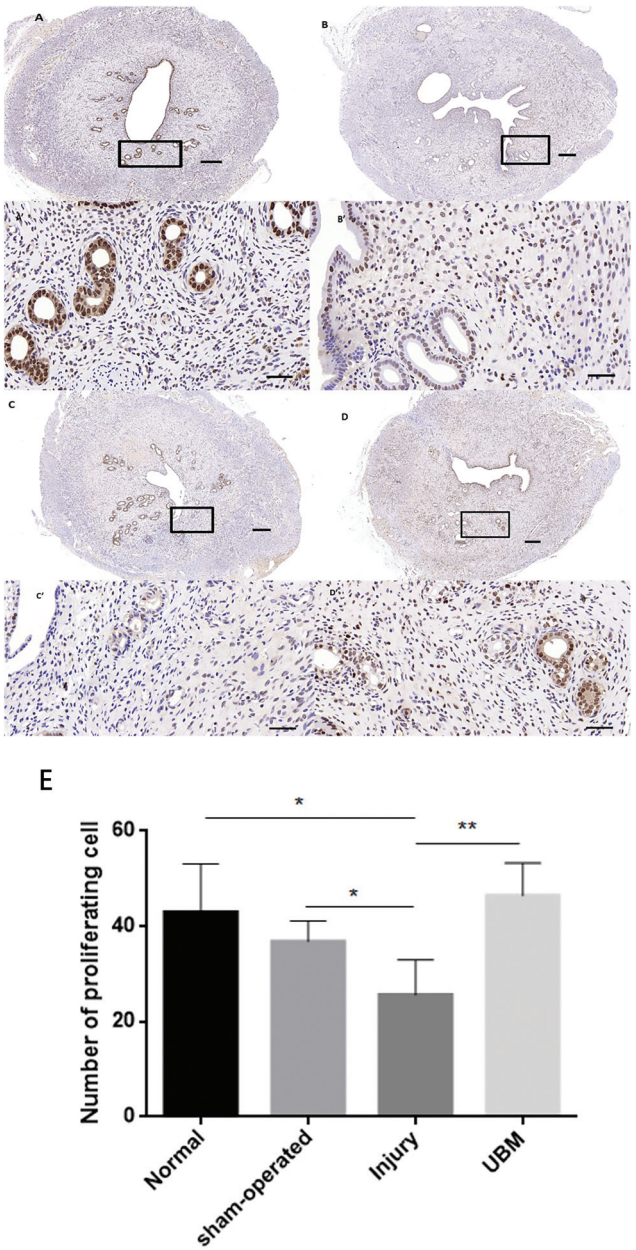

Fig. 6 UBM transplantation increased cell proliferation. Immunohistochemical staining of Ki67 as a marker of cell proliferation in the endometrium at 4 weeks after surgery (A to D) in the normal group (A), the sham-operated group (B), the injury group (C) and the UBM group (D). The scale bars indicate 200 μm (A to D, ×50) or 50 μm (A′ to D′, ×400). (E) Statistical analysis of the number of proliferating cells found in at least 3 randomly selected fields at a magnification of ×400. The data are presented as the mean ± SD; *p < 0.05 and **p < 0.01.

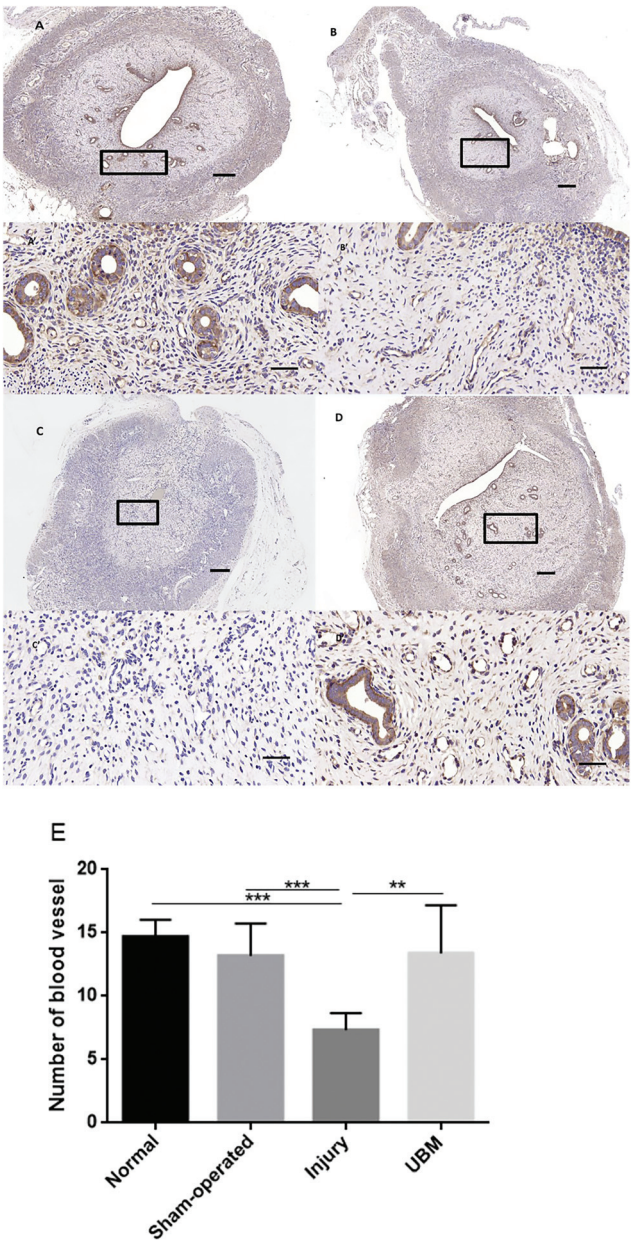

Fig. 7 UBM transplantation increased blood vessel distribution in the endometrium. Immunohistochemical staining of blood vessel (vWF) distribution in the endometrium at 4 weeks after surgery (A to D) in the normal group (A), the sham-operated group (B), the injury group (C) and the UBM group (D). The scale bars indicate 200 μm (A to D, ×50) or 50 μm (A′ to D′, ×400). Statistical analysis of the number of blood vessels found in 3 randomly selected fields at a magnification of ×400 (E). The data are presented as the mean ± SD; **p < 0.01 and ***p < 0.001.

3.5 Endometrial receptivity and pregnancy outcome

Integrin $\alpha V\beta_3$ and leukemia inhibitory factor (LIF) are currently recognized as indicators of endometrial receptivity.[27–29] At 8 weeks after surgery (on the 5th day of pregnancy), as shown in Fig. 9, the mRNA expression of integrin $\alpha V\beta_3$ and LIF was higher in the UBM group than in the injury group. However, the mRNA expression of integrin $\alpha V\beta_3$ and LIF was lower in the UBM group than in the normal and sham-operated groups.

Finally, we determined the effect of UBM transplantation on pregnancy. At 8 weeks after surgery, implanted embryos were found in some of the uterine horns with IUAs (Fig. 9). The number of fetuses in the UBM group (2.1 ± 2.0) was significantly greater than that in the injury group (0.3 ± 0.7);

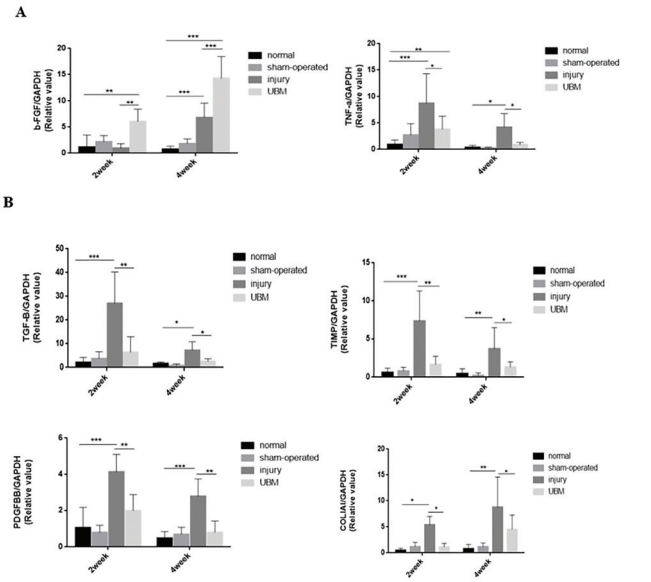

Fig. 8 UBM transplantation enhanced the anti-inflammatory cytokine expression and reduced the proinflammatory and fibrosis-related cytokine expression. The mRNA expression of cytokines in the uterine tissue of the experimental groups was assayed by qRT-PCR. (A) Increased mRNA levels of the anti-inflammatory cytokine bFGF and decreased mRNA levels of the proinflammatory cytokine TNFα were observed in the UBM group compared to the injury group at both 2 weeks and 4 weeks after surgery. (B) Fibrosis-related cytokines (namely, TGFβ, TIMP, PDGF-BB, and COL1A1) were significantly downregulated in UBM-transplanted uteri compared to the injury group. $*p < 0.05$, $**p < 0.01$ and $***p < 0.001$.

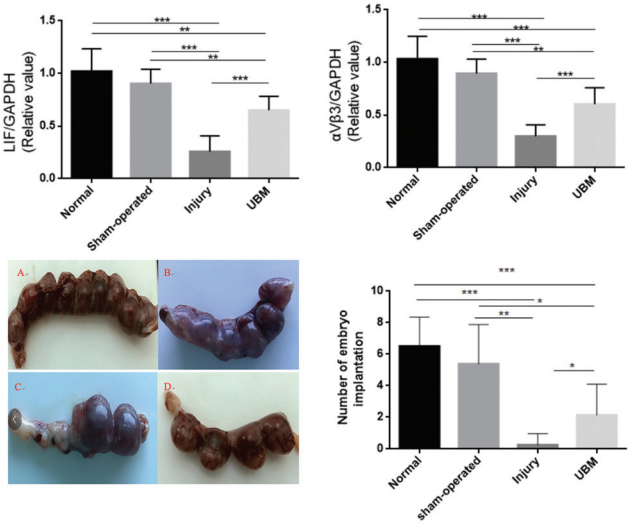

Fig. 9 UBM transplantation increased the pregnancy. Pregnancy of different groups at 8 weeks postoperative in the normal group (A), the sham-operated group (B), the injury group (C) and the UBM group (D). The number of fetuses in the UBM group was greater than that in the injury group; however, it was lower than that in the normal group and in the sham-operated group. $**p < 0.01$ and $***p < 0.001$.

however, it was lower than that in the normal group (6.5 ± 1.9) and in the sham-operated group (5.4 ± 2.5) (Fig. 9).

4. Discussion

Although IUAs were described as early as 1849, regeneration of the endometrium with correct morphology and function in patients with IUAs or thin endometrium is still largely unsuccessful, and IUA remains one of three currently unsolved clinical problems in reproductive medicine. Current research on endometrial regeneration primarily focuses on stem cell therapy, including the use of bone marrow mesenchymal stem cells, embryonic stem cells, menstrual stem cells, and other types of stem cells.[30–32] However, tissue engineering provides another option for endometrial repair.

The ECM is a very complex dynamic system *in vivo*. It not only acts as a biological scaffold that is necessary for the regeneration and repair of tissues and organs but also plays a regulatory role in collective self-repair by releasing important signaling molecules.[33] Tissue-engineered biological scaffolds derived from mammalian ECMs have been shown to have good long-term clinical effects in the reconstruction of damaged tissues and organs.[34] To date, ECMs have been successfully used in the cardiovascular, genital, musculoskeletal, respiratory and gastrointestinal systems and in the treatment of more than 2 million patients.[35–39] Commonly used ECM scaffold materials include Small Intestine Submucosa (SIS), acellular dermis matrix (ADM,) and UBM. Compared to SIS and ADM, UBM has stronger antibacterial activity, better tissue compatibility and hydrophilicity, and better biomechanical properties, biological activity and tissue regeneration induction.[26]

In this study, we induced endometrial injury in rats by mechanical injury. We then implanted UBM biomaterials in rat uteri with damaged endometrium. Through histological study, we found that UBM is rapidly degraded after implantation in the rat uterus and that the UBM is compatible with the surrounding tissue. Two weeks after the surgery, we found that the UBM biomaterial had changed from its membranous form to a milky liquid, and four weeks after surgery, the UBM biomaterial appeared to be almost completely degraded. In the UBM repair group, the thickness of the endometrium and the number of endometrial glands and blood vessels were significantly higher than the thickness and number observed in the injury group and comparable to the thickness and number observed in the normal control group and the sham operation group. This result suggests that UBM may promote the regeneration of the endometrium. This was confirmed by the enhanced levels of bFGF and VEGF observed in the UBM group compared to the injury group. Previous studies have reported that bFGF and VEGF can promote the proliferation and migration of various types of cells, induce neovascularization and participate in tissue repair.[40] Furthermore, studies have shown that bFGF and VEGF play an important role in the repair of the endometrial epithelium, interstitial tissue and angiogenesis.[41,42] Among the more than 5000 peptides and pro-

teins that are degradation products of UBM, 42 have been shown to contribute to tissue regeneration and repair.[43] Moreover, UBM is naturally resistant to infection, possibly due to its rapid rate of neovascularization after implantation in the body and the rapid entry of phagocytic cells into the interior of the material at an early stage, thereby preventing the formation of a bacterial biofilm.[44] These functions of UBM could promote epithelial cell proliferation and migration and inhibit fibrosis. Our data showed that the fibrosis area was decreased after UBM implantation and that the expression of profibrogenic cytokines such as TIMP, PDGFBB, TGF-β, and COLIA1 was consistently reduced.

Endometrial receptivity refers to the ability of the endometrium to accept the embryo. It plays an important role in fertilization and implantation. The endometrium can only accept the embryo during a certain period of the cycle. This optimal time is referred to as the "implantation window" of the embryo. In humans, the implantation window is generally 7–9 days after ovulation,[45] whereas the rat endometrium is capable of receiving embryos within 24 hours of the 5th day after pregnancy.[46] Integrin $\alpha V\beta_3$ is expressed on cell membranes, and the integrins expressed in the embryo and in the endometrium can bind to osteopontin and promote the adhesion of the embryo to the endometrium.[47] The expression of integrin $\alpha V\beta_3$ is spatiotemporally specific, and its expression coincides with the implantation window. LIF is a secreted glycoprotein expressed in endometrial luminal epithelial cells and glandular epithelial cells, and its expression also coincides with the implantation window.[27] Therefore, integrin $\alpha V\beta_3$ and LIF are currently considered to be indicators of endometrial receptivity. Our results showed that the expression of integrin $\alpha V\beta_3$ and LIF was significantly higher in the UBM repair group than in the injury group on the 5th day of pregnancy in rats. The final pregnancy outcome also showed that the pregnancy rate and the number of implanted embryos were significantly higher in the UBM group than in the injury group. These results demonstrate that the endometrium regenerated with the UBM material has good function and that it can restore fertility to some extent.

5. Conclusion

In summary, we have shown that UBM promotes functional repair of the endometrium by promoting the migration and proliferation of endometrial cells and the formation of new blood vessels, thereby improving endometrial receptivity and increasing fertility. UBM implantation has the potential to become a new treatment for patients with IUAs, but more experiments are needed.

Author contributions

WL, FY, and JZ conceived and designed the experiments. HZ and QZ performed the experiments and analyzed the data. HZ wrote the main manuscript. FS prepared the tables, and SW revised the manuscript. All authors reviewed the manuscript.

Conflicts of interest

There are no conflicts to declare.

Acknowledgements

This study was supported by the National Key R&D Program of China (2018YFC1002802 and 2017YFC1001404), the National Natural Science Foundation of China (81873821), the Medical Guidance Project of Shanghai Science and Technology Commission (16411963500) and the Standard Project of Shanghai Science and Technology Commission (16DZ0500402). The authors thank the Department of Medical Genetics and the Animal Experiment Center of the Second Military Medical University for technical support. All animal procedures were performed in accordance with the Guidelines for Care and Use of Laboratory Animals of the Second Military Medical University and approved by the Animal Ethics Committee of the Second Military Medical University.

Notes and references

1 R. F. Casper, *Fertil. Steril.*, 2011, **96**, 519–521.
2 D. Yu, Y. M. Wong, Y. Cheong, E. Xia and T. C. Li, *Fertil. Steril.*, 2008, **89**, 759–779.
3 R. Deans and J. Abbott, *J. Minim. Invasive Gynecol.*, 2010, **17**, 555–569.
4 L. Aghajanova, J. Hoffman, E. Mok-Lin and C. N. Herndon, *Reprod. Sci.*, 2017, **24**, 428–434.
5 E. A. Evans-Hoeker and S. L. Young, *Semin. Reprod. Med.*, 2014, **32**, 392–401.
6 A. Conforti, C. Alviggi, A. Mollo, G. De Placido and A. Magos, *Reprod. Biol. Endocrinol.*, 2013, **11**, 118.
7 C. M. March, *Reprod. Biomed. Online*, 2011, **23**, 63–76.
8 A. E. G. Surgery, *Gynecol. Surg.*, 2017, **14**, 6.
9 C. Simon, *Fertil. Steril.*, 2012, **98**, 1–2.
10 I. Cervelló, A. Mas, C. Gil-Sanchis, L. Peris, A. Faus, P. T. Saunders, H. O. Critchley and C. Simón, *PLoS One*, 2011, **6**, e21221.
11 W. N. Sivak, E. J. Ruane, S. J. Hausman, J. P. Rubin and A. M. Spiess, *Plast. Reconstr. Surg. Global Open*, 2016, **4**, e1094.
12 B. M. Sicari, J. P. Rubin, C. L. Dearth, M. T. Wolf, F. Ambrosio, M. Boninger, N. J. Turner, D. J. Weber, T. W. Simpson, A. Wyse, E. H. Brown, J. L. Dziki, L. E. Fisher, S. Brown and S. F. Badylak, *Sci. Transl. Med.*, 2014, **6**, 234ra258.
13 H. Kimmel, M. Rahn and T. W. Gilbert, *J. Am. Col. Certif. Wound Spec.*, 2010, **2**, 55–59.
14 A. Lanteri Parcells, B. Abernathie and R. Datiashvili, *Wounds*, 2014, **26**, 189–196.
15 L. Gan, H. Duan, F. Q. Sun, Q. Xu, Y. Q. Tang and S. Wang, *Int. J. Gynaecol. Obstet.*, 2017, **137**, 116–122.
16 M. I. Amer, K. Abd-El-Maeboud and A. Alloub, *Middle East Fertil. Soc. J.*, 2012, **17**, 54–56.

17 L. Ding, X. Li, H. Sun, J. Su, N. Lin, B. Peault, T. Song, J. Yang, J. Dai and Y. Hu, *Biomaterials*, 2014, **35**, 4888–4900.
18 N. Lin, X. Li, T. Song, J. Wang, K. Meng, J. Yang, X. Hou, J. Dai and Y. Hu, *Biomaterials*, 2012, **33**, 1801–1807.
19 T. Song, X. Zhao, H. Sun, X. Li, N. Lin, L. Ding, J. Dai and Y. Hu, *Tissue Eng., Part A*, 2015, **21**, 353–361.
20 X. Li, H. Sun, N. Lin, X. Hou, J. Wang, B. Zhou, P. Xu, Z. Xiao, B. Chen, J. Dai and Y. Hu, *Biomaterials*, 2011, **32**, 8172–8181.
21 D. Kong, L. Zhang, X. Xu, J. Zhang, Y. Li and X. Huang, *Gynecol. Obstet. Invest.*, 2018, **83**, 499–507.
22 B. Brown, K. Lindberg, J. Reing, D. B. Stolz and S. F. Badylak, *Tissue Eng.*, 2006, **12**, 519–526.
23 J. C. Schittny and P. D. Yurchenco, *Curr. Opin. Cell Biol.*, 1989, **1**, 983–988.
24 J. Lecheminant and C. Field, *J. Wound Care*, 2012, **21**, 476, 478–480, 482.
25 I. L. Valerio, P. Campbell, J. Sabino, C. L. Dearth and M. Fleming, *Regener. Med.*, 2015, **10**, 611–622.
26 L. Liu, D. Li, Y. Wang, H. Xu, L. Ge and Z. Liang, *Int. Urogynecol. J.*, 2011, **22**, 221–227.
27 E. Hasegawa, H. Ito, F. Hasegawa, K. Hatano, M. Kazuka, S. Usuda and K. Isaka, *Fertil. Steril.*, 2012, **97**, 953–958.
28 G. Chen, A. Xin, Y. Liu, C. Shi, J. Chen, X. Tang, Y. Chen, M. Yu, X. Peng, L. Li and X. Sun, *J. Transl. Med.*, 2016, **14**, 303.
29 D. Zhang, J. Wei, J. Wang, S. Liu, X. Wang and Q. Yan, *Fertil. Steril.*, 2011, **95**, 1446–1451.
30 C. E. Gargett and L. Ye, *Fertil. Steril.*, 2012, **98**, 11–20.
31 C. B. Nagori, S. Y. Panchal and H. Patel, *J. Hum. Reprod. Sci.*, 2011, **4**, 43–48.
32 J. Tan, P. Li, Q. Wang, Y. Li, X. Li, D. Zhao, X. Xu and L. Kong, *Hum. Reprod.*, 2016, **31**, 2723–2729.
33 M. B. Fisher and R. L. Mauck, *Tissue Eng., Part B*, 2013, **19**, 1–13.
34 A. Atala, S. B. Bauer, S. Soker, J. J. Yoo and A. B. Retik, *Lancet*, 2006, **367**, 1241–1246.
35 S. F. Badylak, D. O. Freytes and T. W. Gilbert, *Acta Biomater.*, 2009, **5**, 1–13.
36 N. F. Davis, B. B. McGuire, A. Callanan, H. D. Flood and T. M. McGloughlin, *J. Urol.*, 2010, **184**, 2246–2253.
37 R. S. Howell, M. Fazzari, P. Petrone, A. Barkan, K. Hall, M. J. Servide, M. F. Anduaga and C. E. M. Brathwaite, *JSLS*, 2018, **22**, e2017.00100.
38 A. K. Mahajan, M. Newkirk, C. Rosner and S. J. Khandhar, *J. Surg. Case Rep.*, 2018, **2018**, rjy187.
39 R. G. Frykberg, S. M. Cazzell, J. Arroyo-Rivera, A. Tallis, A. M. Reyzelman, F. Saba, L. Warren, B. C. Stouch and T. W. Gilbert, *J. Wound Care*, 2016, **25**(Suppl 7), S18–S25.
40 S. T. Nillesen, P. J. Geutjes, R. Wismans, J. Schalkwijk, W. F. Daamen and T. H. van Kuppevelt, *Biomaterials*, 2007, **28**, 1123–1131.
41 P. Wei, X. L. Chen, X. X. Song, C. S. Han and Y. X. Liu, *Mol. Reprod. Dev.*, 2004, **68**, 456–462.
42 C. E. Gargett, R. W. Chan and K. E. Schwab, *Mol. Cell. Endocrinol.*, 2008, **288**, 22–29.
43 H. Marçal, T. Ahmed, S. F. Badylak, S. Tottey and L. J. Foster, *Regener. Med.*, 2012, **7**, 159–166.
44 A. G. Harrell, Y. W. Novitsky, K. W. Kercher, M. Foster, J. M. Burns, T. S. Kuwada and B. T. Heniford, *Hernia*, 2006, **10**, 120–124.
45 H. J. Lim and S. K. Dey, *Exp. Cell Res.*, 2009, **315**, 619–626.
46 A. M. Sharkey and S. K. Smith, *Best Pract. Res. Clin. Obstet. Gynaecol.*, 2003, **17**, 289–307.
47 R. Nejatbakhsh, M. Kabir-Salmani, E. Dimitriadis, A. Hosseini, R. Taheripanah, Y. Sadeghi, Y. Akimoto and M. Iwashita, *Reprod. Biol. Endocrinol.*, 2012, **10**, 46.